Assessment of Differential Protection Applied to LCC-HVDC Converter Transformers

Glaufe S. Oliveira, Kleber M. Silva

***Abstract*—This paper presents an analysis of the performance of phase and negative-sequence differential protection functions (87T and 87Q) of converter transformers that are connected in the inverter station of line-commutated converter (LCC) high-voltage direct current (HVDC) systems. The study investigates the behavior of these protections during external faults in the AC system, transformer energization, and internal faults. The LCC-HVDC Madeira River link system was modeled using the ATP/ATPDraw software to simulate the scenarios and assess the responses of the protection functions. The results reveal that the 87T and 87Q functions effectively protected transformers during energization, external faults, and internal primary-side faults. However, current signal distortion results of turn-to-ground and single-phase-to-ground faults in the transformers' DC side can lead to differential protection malfunction, including non-operation for internal faults due to improper blocking and restriction by 2nd harmonic or inadequate functions' sensitivity. Despite these limitations, the 87Q function showed promise for protecting specific converter transformers. Hence, enhancements are needed to address DC-side fault challenges, with future research focusing on better energization detection and tailored protection schemes for HVDC converter transformers. Moreover, the results of turn-to-ground faults are sufficient and more comprehensive in explaining the challenges encountered. Therefore, they are the focus of this paper.**

***Keywords*—ATP, converter transformers, electromagnetic transients, LCC-HVDC, negative-sequence differential protection, phase differential protection.**

I. Introduction

CONVERTERS transformers are an essential part of HVDC systems [1], [2] and are costly to produce and transport due to their large size, resulting in extended replacement periods in equipment loss or relatively long maintenance periods in the event of breakdowns [2], [3]. Therefore, protecting these devices is a fundamental part of the overall HVDC system protection strategy, making targeted studies of their specific protection requirements crucial.

Despite the unique aspects of converter transformers, their fundamental operation is directly comparable to conventional transformers, and their protection generally utilizes traditional differential protection functions [2], [3]. However, since differential protection fundamentally compares the transformer terminals' currents, the connection to the DC system may or may not negatively impact the performance of these protections, and investigating this impact is crucial.

Glaufe Santos de Oliveira is with the National Electric System Operator (ONS), Rio de Janeiro, Brazil (e-mail: glaufe.oliveira@ons.org.br).

Kleber Melo e Silva is with the University of Brasilia (UnB), Brasilia, Brazil (e-mail: klebermelo@lapse.unb.br).

Paper submitted to the International Conference on Power Systems Transients (IPST2025) in Guadalajara, Mexico, June 8-12, 2025.

As a result, a few studies have been conducted explicitly addressing the phase differential protection of HVDC converter transformers (ANSI code 87T) [2], [4]-[8].

In [2], the behavior of phase differential protection with harmonic blocking was evaluated for internal faults in converter transformers. For this purpose, the CIGRE HVDC benchmark test system in PSCAD/EMTDC was used to simulate the faults, and the differential protection was modeled to respond to the simulation results. As a result, [2] identified the occurrence of undue blocking of the differential protection in the occurrence of asymmetric internal ground faults on the DC side of the converter transformers. According to the analyses performed, the blocking occurred due to a significant value of the DC component in the fault currents that flowed through the fault point and caused a half-cycle saturation in the converter transformers, which led to an increase in the 2nd harmonic component in the transformer currents. Thus, the differential protection was blocked due to the 2nd harmonic component exceeding the blocking limit.

In [4], the use of the 2nd harmonic was evaluated to identify energization in the converter transformers. To this end, simulations based on RTDS were performed using a model of the 800 kV Chusui HVDC link and simulations of the response of the 87T function with 2nd harmonic blocking. The following scenarios were verified: energization of the transformers at no load, single-phase-to-ground fault in the secondary, phase-to-phase-to-ground fault in the secondary, and three-phase-to-ground fault in the secondary. Thus, false trips for energizing the transformers were verified due to failure in the 2nd harmonic blocking and non-actuation for the faults evaluated due to the presence of the 2nd harmonic.

In [5] and [6], the operation of an HVDC converter rectifier was analyzed during single-phase-to-ground faults in the converter transformer valve side using an HVDC model in PSCAD/EMTC. It verified the occurrence of fault-induced inrush current (FIIC). During the fault, an increase in the DC current in the transformer is observed, which led the transformer voltage to generate an aperiodic offset and contributed to a half-cycle saturation in its core, resulting in a high 2nd harmonic current. Therefore, [5] observed a delay in the protection operation for internal faults and undue blocking by the 2nd harmonic for transferred faults from external to internal. At the same time, [6] confirmed the undue blocking in the differential protections due to a 2nd harmonic current and verified that for star-star converter transformers, FIICs happen in the three phases of the transformer. In contrast, for star-delta transformers, FIIC occurs only in two phases.

In [7], the FIICs and their impact on the differential protection of converter transformers were also analyzed, but this time, on the transformers on the inverter station of an HVDC link. Moreover, an HVDC model in PSCAD/EMTC was also used for simulations. As a result, [7] noticed that the fault current on the valve side of the transformer after a single-phase-to-ground fault depends mainly on the conduction states of the common anode thyristors and in which transformer of the bipole/pole the fault occurred. Furthermore, still for single-phase-to-ground faults, a protection delay for internal faults on the valve side was verified, and non-actuation was observed for transferred faults on the valve side. Both occurred due to blocking by 2nd harmonic currents.

In [8], the 87T function and the transformer negative-sequence differential protection function (ANSI code 87Q) were analyzed under limited scenarios, and preliminary results revealed performance issues. Although [8] did not identify the causes of these failures, it confirmed that high levels of 2nd harmonics were present in the operating currents for internal faults.

Hence, in this paper, a complete analysis of the current differential functions for transformers will be carried out, from 87T to 87Q functions. Unlike the works already published on the topic and referenced in this section, this paper goes beyond evaluating single-phase-to-ground faults and improper blocking by the 2nd harmonic. It evaluates several scenarios and delves into the effectiveness of differential functions for turn-to-ground faults in their various possibilities and for different converter transformers of an HVDC system. It verifies that improper blocking by the 2nd harmonic is not the only challenge for protecting this equipment and that just a new way of detecting the energization of these transformers may not be enough to solve the problems encountered. In addition, based on the research carried out and the challenges already verified and signaled in the referenced works, this article also evaluates the possibility of using the 87Q function as an alternative to aggregate the protection of HVDC converter transformers. Consequently, this work aims to add knowledge to the literature to support deciding which functions and adjustments to use to protect this equipment. Furthermore, to make the most of the paper, the analyses will focus on the problems encountered, while the correct operations of the protections will only be mentioned.

II. Evaluated Power System

The evaluated power system in this paper corresponds to the LCC-HVDC link of Madeira River, which consists of two bipoles with a length of 2,450 km each, a power rating of 3,150 MW each, and ± 600 kV. The link is the second-built Brazilian HVDC system and connects the Porto Velho Collector (CPV) and Araraquara II (AQD) stations, transporting part of the large hydraulic potential of the country's Amazon region to its largest load center. The model representing the system was implemented by [9], based on an LCC-HVDC benchmark model from CIGRE developed in ATP/ATPDraw by [10]. It effectively represents the bipoles' control, closely mirroring real-world conditions, because the benchmark model was built from the PSCAD model of the Madeira River LCC-HVDC link used for planning the bipoles integration into Brazil's electrical system. [9], in turn, improved the model by duplicating the bipole in parallel and adding parts of the adjacent AC system using real system parameters.

Then, in this paper, the converter transformers of the model were replaced by specific saturable transformer models (including their saturation characteristics [11]) that allowed simulations of turn-to-turn and turn-to-ground faults, and current transformers (CTs) were inserted in the transformers for result reading, also considering its saturation characteristics and measurement errors [12].

In Fig. 1, the six-pulse bridges of Bipole 1 inverters are highlighted as Inv_1, Inv_2, Inv_3, and Inv_4, with transformers labeled as $TFYY_1$, $TFYD_1$, $TFYY_2$, and $TFYD_2$. Such distinctions are necessary because, unlike other fault types, the outcomes of turn-to-ground and single-phase-to-ground faults in the secondary depend on the transformers' position within the pole. Another key point is that the connection between Inv_2 and Inv_3 is grounded, enabling bipole operation with positive voltage at 600 kV in V^{+}_{dc} and negative voltage at -600 kV in V^{-}_{dc}.

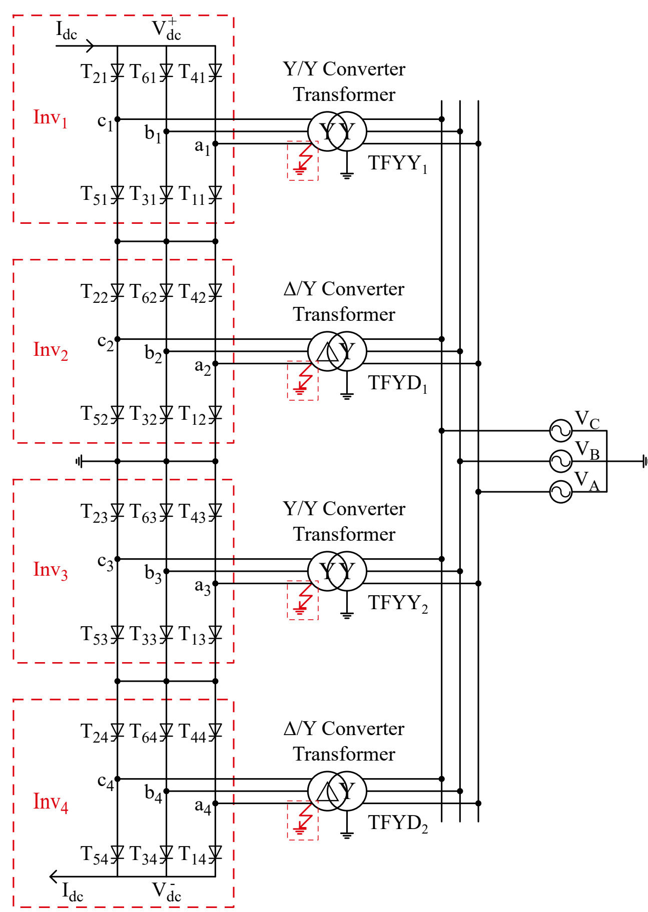

Fig. 1. Diagram of the converter inverter evaluated to short circuits in the secondary of its converter transformers.

The converter transformers' terminals will be considered as the primary side, connected to the AC network, and the secondary side, connected to the converters. Additionally, the configuration of the TFYDs are grounded star on the primary side and delta on the secondary side. In contrast, the TFYYs are grounded star on the primary side and ungrounded star on the secondary side.

III. Simulations Description

To evaluate the functions 87T and 87Q, their logic and the Modified Cosine Filter for phasor estimation proposed by [13] were computationally implemented. After the simulations in ATP/ATPDraw with a simulation step of 2.5 μs, the CTs reading data were conditioned by filtering them with a 3rd-order Butterworth low-pass anti-aliasing filter with a cutoff frequency of 480 Hz, which enabled the filtered signals to be resampled at a rate of 16 samples per 60 Hz cycle to be then estimated and used by the protection functions. This approach enabled the simulation of these functions' behavior as they would operate in a real-world Intelligent Electronic Device (IED). Additionally, the results were analyzed through digital trip signals for each function and the operating current x restraining current plane (I_{op} x I_{res} or I_{adj} in case of restriction by harmonics). In summary, I_{op} indicates the presence of an internal short circuit fault, while I_{res} and I_{adj} prevent incorrect operations. In other words, differential protections are activated when I_{op} exceeds the product of the slope and I_{res} or I_{adj} (where the slope is a sensitivity factor of the relay that defines the percentage of restraint current, indicating the level at which the operating current must surpass to trigger tripping). These currents are calculated by the phase currents in function 87T and by the negative sequence currents for function 87Q, which is an alternative for faults with little impact on the phase currents, causing them not to be sensitized but with an imbalance between the phases.

Blocking and restriction by 2nd and 5th harmonics, on the other hand, are typically used to identify inrush currents (2nd) and over-excitation (5th) in transformers to avoid improper operations caused by these phenomena during normal operations of this equipment, such as the energization of the transformers [3]. Hence, the performance of function 87T was assessed without restrictions or blocking by harmonics, with only restrictions by harmonics (87T R.H.), and with restrictions and blocking by harmonics (87T R.B.H.). At the same time, function 87Q was evaluated with blocking by harmonics and a delay of two cycles to avoid false trips (87Q B.H. DLY) and with only delay (87Q DLY).

The functions' settings were selected based on the available ranges of a commercial transformer relay [14]. They were optimized during the analysis for the best possible performance of the protections in the evaluated system. The minimum pick-up current setting was adjusted to 1 pu of the rated current for the 87T function and 0.1 pu for the 87Q function, and the slope parameter was set to 0.3 for 87T and 0.4 for 87Q. Additionally, the settings for harmonic restraining and blocking were adjusted as follows: a 15% increase in restraining current based on the levels of the 2nd and 5th harmonics and blocking of the functions when the presence of 2nd or 5th harmonics in operating current is greater than or equal 25% about the fundamental.

External and internal faults were evaluated to verify the selectivity and reliability of differential functions. The internal fault scenarios were chosen according to the fault probabilities of converter transformers [2], [15], [16]. The faults evaluated were:

- Turn-to-turn faults taking from 1 to 100% of the turns in both the primary and secondary of the converter transformers.
- Turn-to-ground faults taking from 1 to 100% of the turns in both the primary and secondary of the converter transformers.
- Single-phase-to-ground, phase-to-phase, and phase-to-phase-to-ground faults at converter transformers' primary and secondary terminals.
- Single-phase-to-ground, phase-to-phase, phase-to-phase-to-ground, and three-phase faults at the beginning and middle of an AC transmission line connected to the Araraquara 2 Substation.
- Energization of the converter transformers.

IV. Results and Discussions

The differential functions were effective and operated correctly for all faults analyzed in the transformers' primary. They did not operate for external faults or during transformer energization. For internal faults in the transformer at the secondary terminal, the functions operated correctly only for phase-to-phase, phase-to-phase-to-ground, and turn-to-turn short circuits.

Meanwhile, the turn-to-ground faults and single-phase-to-ground in the secondary of the converter transformers represent the most significant challenge concerning differential protection functions in this work. A malfunction was observed in the 87T and 87Q functions. Additionally, the challenges encountered are sufficiently explained when analyzing the results for turn-to-ground faults, which is this paper's focus. Besides that, all the turn-to-ground faults were applied in phase A.

Starting the discussion with the $TFYY_1$, the function 87T without harmonic restraint or blocking only operated for turn-to-ground faults in its secondary side involving over 56% of turns. In contrast, with harmonic restraint and blocking, the function did not operate for any percentage of turns involved (Fig. 2).

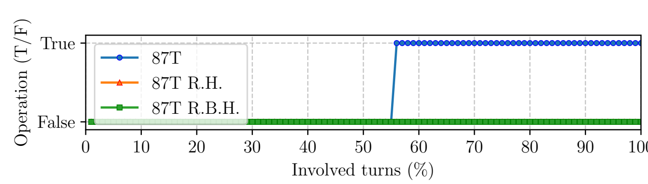

Fig. 2. 87T function operation in $TFYY_1$ for turn-to-ground short circuits on the secondary side.

Additionally, from the same 56% threshold, the 2nd harmonic block is triggered immediately after the fault and persists as long as the fault remains (Fig. 3). As a result, no differential function performs under these conditions. So, when harmonic blocking is applied, the 87T function does not trigger at any percentage. Considering only harmonic restraint, the function again does not operate for any percentage of turns, confirming the high levels of harmonics and their impact on the protection (Fig. 2).

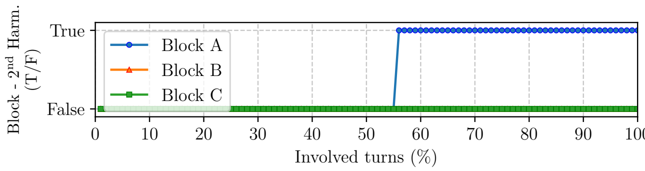

Fig. 3. Blocking by 2nd harmonic for turn-to-ground short circuits in the secondary of the converter transformer $TFYY_1$.

Understanding the inverter post-fault condition is essential to understand the source of the high level of 2nd harmonics. Fig. 4 shows the current in the $TFYY_1$'s during a turn-to-ground short circuit taking 90% of the secondary winding turns, where positive currents correspond to currents from common anode thyristors (T_{21}, T_{61}, and T_{41}) and negative currents correspond to common cathode thyristors (T_{51}, T_{31}, and T_{11}). Through Fig. 4, it is possible to verify that the pole control could adjust to maintain a non-ideal operation. There is only one commutation failure in Inv_1 immediately after the fault (between 0.5 and 0.52 seconds), which is confirmed by the output value from the ATP model used that indicates when there is a commutation failure in the inverter during the simulation.

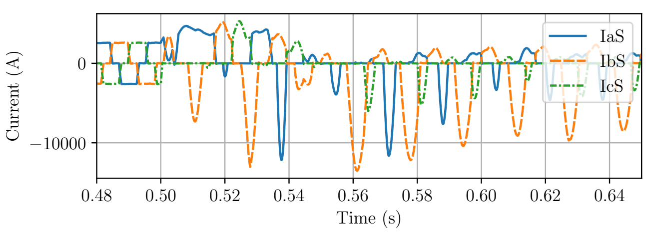

Fig. 4. Currents on the secondary side of $TFYY_1$ during a turn-to-ground short circuit at 90% of the secondary side.

From Fig. 4, it is verified that the inverter continues the thyristor commutation similarly to the regular operation but with three critical differences: increased current due to the short circuit, non-conduction in some common-cathode thyristors, even though they were connected, and more notably, the characteristic shape of an inrush current in the phase currents.

Thyristors of HVDC converters always operate in pairs, so the resulting DC voltage at each inverter terminal corresponds to the phase voltage difference across the secondary of its converter transformer, maintaining either positive or negative DC voltage differences. Consequently, the voltages at each phase of the transformer's secondary side result from the AC system voltage plus the DC voltage from the inverter, depending on which thyristor is conducting in each phase. Due to the grounding from a 90% turn-to-ground fault, the V_a voltage in the secondary drops to nearly zero, though not entirely, due to the remaining 10% of turns between the phase and fault. This configuration creates a sinusoidal behavior of V_a, referenced to phase A's voltage in the AC system. In contrast, V_b and V_c secondary voltages align with the AC system's line voltages, approximating V_{ba} and V_{ca}, respectively, due to the fault's location.

Figs. 5 and 6 depicts the secondary post-fault phase and line voltages of transformer $TFYY_1$, illustrating the aforementioned effects. Furthermore, as thyristor commutation continues, voltage "cuts" are observed at V_a, V_b, and V_c when common-cathode thyristors are turned on, bringing the phase voltage (AC + DC voltage) close to zero, similar to regular operation.

Thus, common-cathode thyristors cease conducting when thyristor pairs T_{21} and T_{11}, and T_{61} and T_{51}, are active, as V_a and V_c enter their negative half-cycles, halting the current flow. However, no commutation failure occurred, as phase voltage was positive at the commutation.

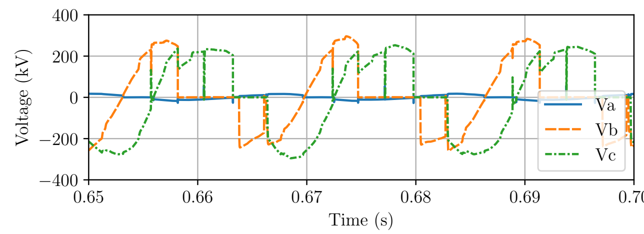

Fig. 5. Post-fault phase voltage for a turn-to-ground short circuit at 90% of the secondary of the converter transformer $TFYY_1$.

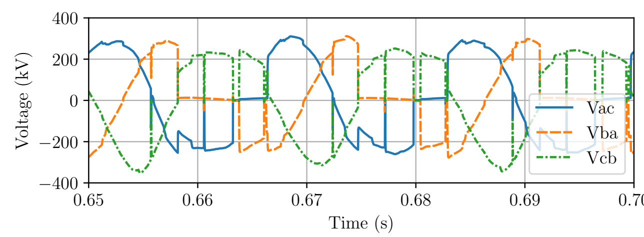

Fig. 6. Post-fault line voltage for a turn-to-ground short circuit at 90% of the secondary of the converter transformer $TFYY_1$.

The fault current on the secondary (Fig. 4) reflects directly on the primary side, as seen in Fig. 7, which shows the current on the primary side during the fault. The currents of phase B and C mirror those in the transformer's secondary side, yet phase A currents display substantial differences. It is verified that the current of phase A on the primary side is never equal to zero, even when there is no current in the phase on the secondary side. This difference is obviously due to the phase connection to ground in 90% of the secondary winding and demonstrates that the fault is continuously fed by the common anode thyristors, as well as demonstrates how the fault causes a continuous flow of DC current in the transformer, causing the core saturation and, as a consequence, the FIIC [5]-[7]. Then, the phase A primary-secondary current differences are detected by the 87T function, as shown in Figs. 2 and 8. However, the current offset in the transformer leads to non-operation of the 87T function due to restriction or inappropriate 2nd harmonic blocking caused by the FIIC.

Fig. 8 shows the 87T function's operation without harmonic blocking, while Fig. 9 displays the function with harmonic restraining and blocking. These figures confirm that both

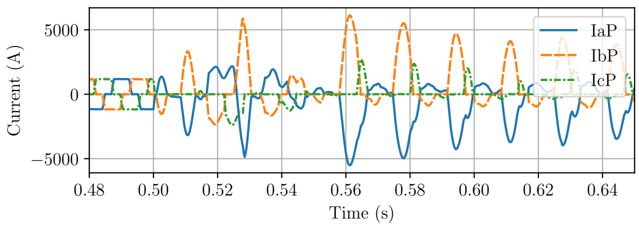

Fig. 7. Currents on the primary side of $TFYY_1$ during a turn-to-ground short circuit at 90% of the secondary side.

restriction and blocking hindered the protection function, which is especially evident in the 2nd harmonic levels and the blocking shown in Fig. 10.

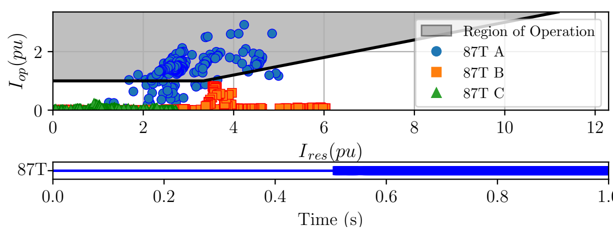

Fig. 8. 87T function operation in $TFYY_1$ for a turn-to-ground short circuit at 90% of the secondary side.

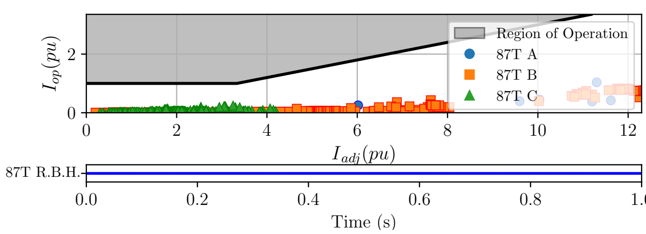

Fig. 9. 87T R.B.H. function operation in $TFYY_1$ for a turn-to-ground short circuit at 90% of the secondary side.

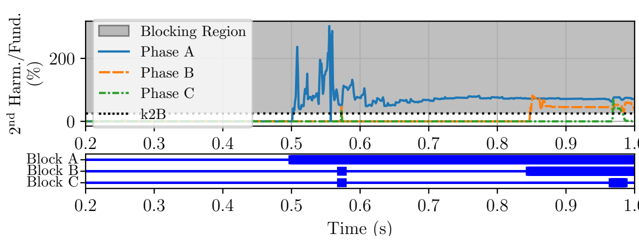

Fig. 10. 2nd harmonic by fundamental for a turn-to-ground short circuit at 90% of the secondary of the converter transformer $TFYY_1$.

The same results are obtained for up to 56% of turns involved in the short circuit, precisely at which the 87T function without blocking or harmonic restraint starts to be activated (Fig. 2).

Even more critical results are found analyzing the 87T function for converter transformer $TFYD_1$: the function does not operate at any percentage of turns, even without harmonic blocking or restraint, as illustrated in Fig. 11. This finding shows that the primary issue for this converter transformer is not harmonic blocking or restraint, which is different from $TFYY_1$. This contrast is confirmed by assessing the blocking for the 2nd and 5th harmonics per percentage of turns in Figs. 12 and 13. There is no function blocking due to harmonic levels. Note that function-blocking in Figs. 12 and 13 was considered for each percentage of turns where blocking was sustained and prevented differential function operation, excluding faults with transient levels of the 2nd and 5th harmonics beyond the limit.

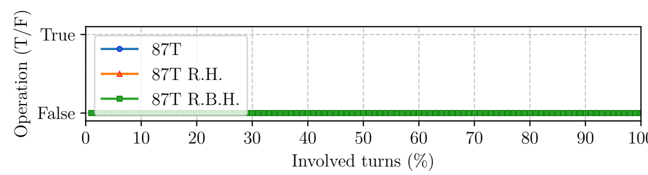

Fig. 11. 87T function operation in $TFYD_1$ for turn-to-ground short circuits on the secondary side.

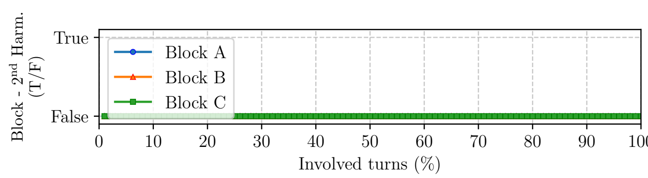

Fig. 12. Blocking by 2nd harmonic for turn-to-ground short circuits in the secondary of the converter transformer $TFYD_1$.

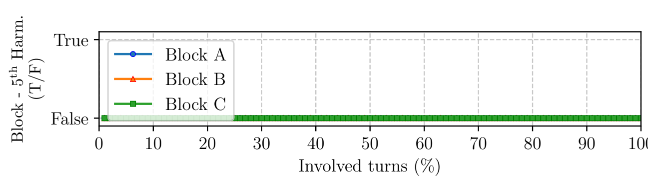

Fig. 13. Blocking by 5th harmonic for turn-to-ground short circuits in the secondary of the converter transformer $TFYD_1$.

It is essential to examine the post-fault configuration of inverter Inv_2 and converter transformer $TFYD_1$ to understand this result and the difference compared to $TFYY_1$ transformer results. It is known that differential functions have difficulty detecting turn-to-ground faults near 50% of a winding [3]. However, as the 87T function does not operate even in the worst cases at winding ends, the analyses will focus on a turn-to-ground fault taking 90% of $TFYD_1$ secondary turns, which exemplifies faults with other percentages of turns.

Figs. 14 and 15 shows the $TFYD_1$ converter transformer's currents after the fault. While turn-to-ground faults on $TFYY_1$ cause few or no commutation failures, $TFYD_1$ faults exhibit a consistent commutation failure pattern throughout the fault. This difference is critical, as after commutation failures happen just in the Inv_2, the pole can be tripped by Commutation Failure Protection [3], whereas $TFYY_1$ faults rely on other protections to identify or not the fault.

The commutation failures of Inv_2 occur during the commutation from T_{41} to T_{61} and from T_{51} to T_{11}. After the fault, voltages V_a, V_b, and V_c also exhibit a sinusoidal behavior, as shown in Figs. 16 and 17, which displays the phase and line voltages at the transformer's secondary side before and after the fault. This fault also resulted in a commutation shift among the thyristors to the point that the

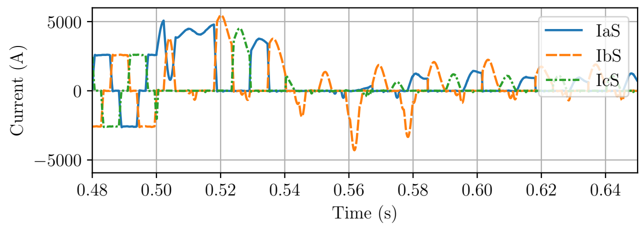

Fig. 14. Currents on the secondary side of $TFYD_1$ during a turn-to-ground short circuit at 90% of the secondary side.

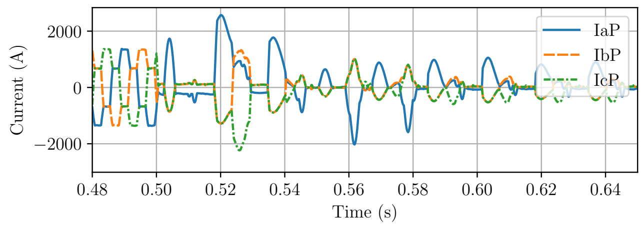

Fig. 15. Currents on the primary side of $TFYD_1$ during a turn-to-ground short circuit at 90% of the secondary side.

commutation attempt from T_{41} (phase A) to T_{61} (phase B) and from T_{51} (phase C) to T_{11} (phase A) occurs when V_b is lower than V_a and V_c is lower than V_a, respectively, causing the commutation failures. Additionally, non-conduction in the common cathode thyristors occurs for the same reason observed in previous cases. Even when commutation does occur, the phase voltages remain negative.

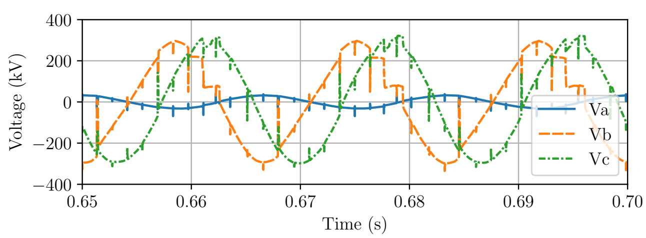

Fig. 16. Post-fault phase (a) and line (b) voltage for a turn-to-ground short circuit at 90% of the secondary of the converter transformer $TFYD_1$.

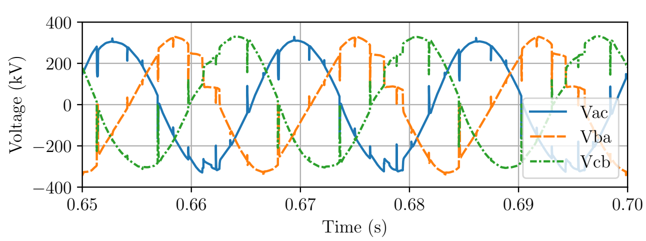

Fig. 17. Post-fault phase (a) and line (b) voltage for a turn-to-ground short circuit at 90% of the secondary of the converter transformer $TFYD_1$.

Consequently, the currents are reflected coherently on the primary, except for the phase-a current (Fig. 15). However, given the reduced current values and the filtering of the DC component during phasor estimation, the phase-A operating current is insufficient to sensitize the 87T function, as demonstrated in Fig. 18.

Fig. 19 shows the 2nd harmonic blocking for this fault. It is evident that DC current effects in the transformer still lead to increased harmonics, particularly in the 2nd harmonic component. However, there is no sustained blocking due to harmonic levels, and the function does not operate strictly due to a lack of sensitivity.

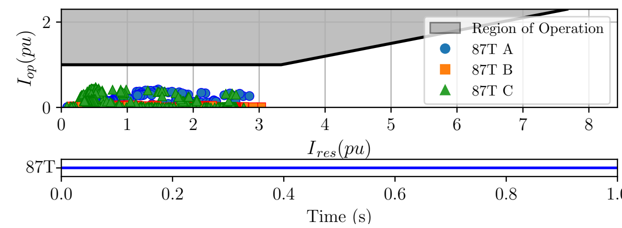

Fig. 18. 87T function operation in $TFYD_1$ for a turn-to-ground short circuit at 90% on the secondary side.

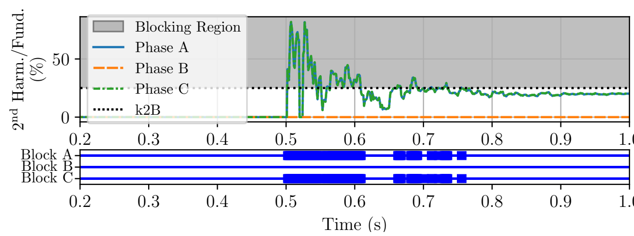

Fig. 19. 2nd harmonic by fundamental for a turn-to-ground short circuit at 90% of the secondary of the converter transformer $TFYD_1$.

Finally, it is essential to clarify that the differences in results between $TFYY_1$ and $TFYD_1$ are not due to the configuration differences between the converter transformers, that is, star-star and star-delta. Besides the reasons already stated, the lower currents and differences in $TFYD_1$ result from its position in the pole. Turn-to-ground short circuits in $TFYD_1$ significantly impact $TFYY_1$ and, consequently, the pole as a whole, considering that the phase voltages in $TFYY_1$ are the sum of the AC voltage plus the DC voltage resulting from Inv_2. As demonstrated in Fig. 1, the line DC voltage of the poles is equivalent to the sum of the terminal voltages of each six-pulse converter. In other words, the voltage V^{+}_{dc} is equal to the sum of the voltage of the inverters Inv_1 and Inv_2, with reference ($V = 0$) in the connection to the neutral between the inverters Inv_2 and Inv_3, while the voltage V^{-}_{dc} is equal to the sum of the terminal voltages of Inv_3 and Inv_4. Accordingly, the operation of the inverters Inv_1 and Inv_4 depends on the terminal voltage of the inverters Inv_2 and Inv_3, respectively. So, single-phase-to-ground and turn-to-ground faults in the secondary of the converter transformers connected to $InvInv_2$ and $InvInv_3$ cause a voltage drop and impact not only on these inverters but also on the inverter above. Therefore, since the fault current naturally depends on the voltage connected to the fault and the impedance of the fault equivalent circuit, and the voltage for faults in the secondary of converter transformers comes mainly from the DC system, such faults result, together with the response of the inverter control, in the lower fault currents observed in Fig. 14. Nevertheless, faults in the DC-side of converter transformers connected to the inverters Inv_1 and Inv_4 do not cause the same effect. The fault voltage corresponds more directly to the pole line voltage, V^{-}_{dc} or V^{-}_{dc}, which causes higher fault currents that, as a result, sensitize the 87T function but also increase the FIICs and cause the blocking and restriction of the functions.

These effects can be seen in Fig. 20, which shows secondary currents in $TFYY_1$ for a turn-to-ground fault taking 90% of turns in $TFYD_1$. The figure shows that currents in $TFYY_1$ are reduced to peak values of 450 and 600 A at brief moments. In the opposite case shown in Fig. 21, $TFYD_1$ currents maintain the pattern according to thyristor commutation, with values between 1000 and 2000 A, while in regular operation, the currents maintained a value of 2625 A for 100% of power transmission.

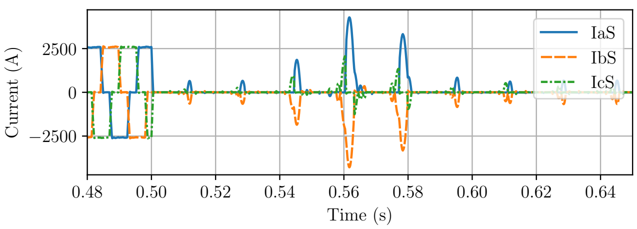

Fig. 20. Currents on the secondary side of $TFYY_1$ during a turn-to-ground short circuit at 90% of the secondary side of $TFYD_1$.

To confirm the results, a turn-to-ground short circuit taking 90% of turns in the secondary of the converter transformers $TFYY_2$ and $TFYD_2$ was also evaluated——the results aligned with expectations relating to pole position and not transformer connection. Figs. 22 and 23 show the secondary currents of transformers $TFYY_2$ and $TFYD_2$ for short circuits at 90% of their turns. Compared with the results of transformers $TFYY_1$ (Fig. 4) and $TFYD_1$ (Fig. 14), it becomes evident how the result depends on the transformer location in the pole. However, corroborating the results of [6], in $TFYD_2$, the FIIC occurs only in two phases, while in $TFYY_1$, it occurs in all three.

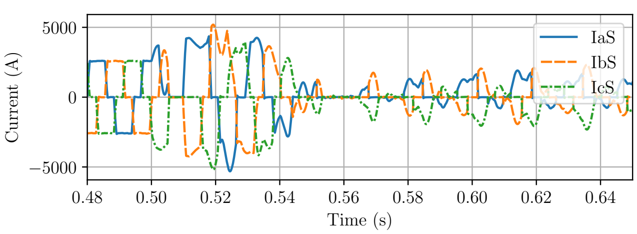

Fig. 21. Currents on the secondary side of $TFYD_1$ during a turn-to-ground short circuit at 90% of the secondary side of $TFYY_1$.

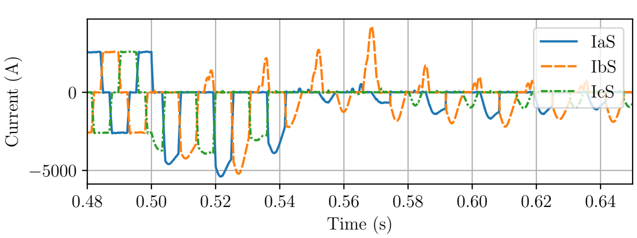

Fig. 22. Currents on the secondary side of $TFYY_2$ during a turn-to-ground short circuit at 90% of the secondary side.

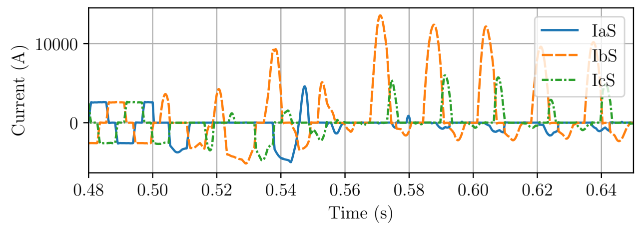

Fig. 23. Currents on the secondary side of $TFYD_2$ during a turn-to-ground short circuit at 90% of the secondary side.

In addition to the factors analyzed before, two other details already partially discussed impact fault identification by the differential functions. The first is how the AC system perceives the DC system as a high impedance, as the poles directly control the currents in the transformers, preventing the fault from being fed by the AC system. Thus, the fault result follows as detailed before, where the current of the transformer depends on the inverters. Along the same lines, the second detail concerns the converter control response to the fault, which aims to maintain bipole stability and operation so that the fault current is limited and sometimes reduced after the initial fault current transient.

All these points also affect the 87Q function, so the results of the 87Q match Figs. 24 and 25. 87Q function does not prove helpful for $TFYY_1$ beyond the 87T function, which occurs due to the behavior after the fault in the transformer, where for a fault of 55% of turns or less, the currents of the transformer maintain a pattern controlled by the pole control. Therefore, even with the offset, the phase imbalance occurs only momentarily and transiently at the fault moment, and the 87Q function is prevented from operating by the delay. For faults above this percentage of turns, the 87T function already identifies the fault, and the harmonic level blocks both equally.

As for the converter transformer $TFYD_1$, even with the delay, the function proves useful and serves as a backup for the 87T function. As verified in Fig. 14 and previously detailed, a turn-to-ground short circuit in the secondary of $TFYD_1$ causes such an impact on the inverter that it leads to phase imbalance. However, as expected for a star-delta transformer, the function performs more consistently at the ends of the windings. To better visualize the result, Fig. 26 shows the operation of the 87Q function for a fault taking 10% of the turns.

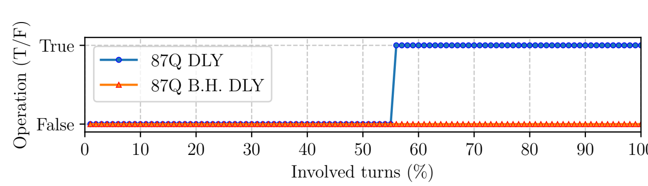

Fig. 24. 87Q DLY function operation in $TFYY_1$ for turn-to-ground short circuits on the secondary side.

For a better understanding of the results and the advantages and disadvantages of using the differential functions analyzed in this paper, the results obtained were summarized in tables. Table I summarizes the incorrect operations in transformers $TFYY_1$ and $TFYD_1$, except results for turn-to-ground faults,

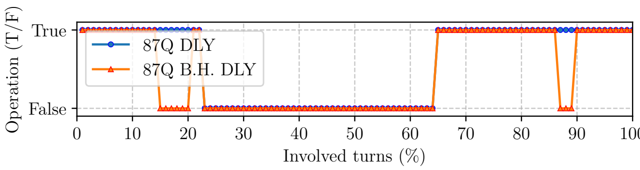

Fig. 25. 87Q DLY function operation in $TFYD_1$ for turn-to-ground short circuits on the secondary side.

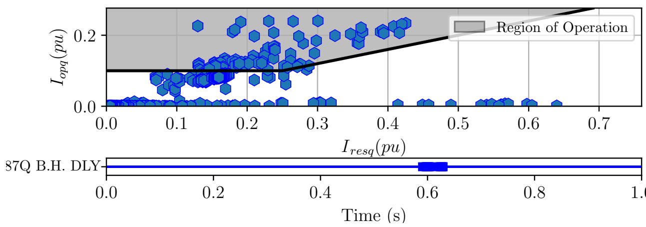

Fig. 26. 87Q function operation in $TFYD_1$ for a turn-to-ground short circuit at 10% of the secondary side.

which are summarized in Tables II and III that indicate which functions performed correctly (✓) or not (×), considering that they are more specific and need to be detailed.

TABLE I
INCORRECT OPERATION SUMMARY FOR $TFYY_1$ AND $TFYD_1$.

Case	Incorrect Operations	
	$TFYY_1$	$TFYD_1$
Energization	87T / 87Q DLY	87T / 87Q DLY
External Faults	None	None
Primary Side Faults	None	None
Secondary Side Faults	87T R.B.H. and 87Q B.H. DLY for Single-phase-to-ground faults	87T and 87T R.B.H. for Single-phase-to-ground faults

TABLE II
87T AND 87Q FUNCTION OPERATION SUMMARY FOR TURN-TO-GROUND SHORT CIRCUITS IN THE SECONDARY OF $TFYY_1$.

Turns (%)	87T	87T R.B.H.	87Q DLY	87Q B.H. DLY
1 to 55 %	×	×	×	×
56 to 100 %	✓	×	✓	×

TABLE III
87T AND 87Q FUNCTION OPERATION SUMMARY FOR TURN-TO-GROUND SHORT CIRCUITS IN THE SECONDARY OF $TFYD_1$.

Turns (%)	87T	87T R.B.H.	87Q DLY	87Q B.H. DLY
1 to 14 %	×	×	✓	✓
15 to 20 %	×	×	✓	×
21 to 22 %	×	×	✓	✓
23 to 64 %	×	×	×	×
65 to 86 %	×	×	✓	✓
87 to 89 %	×	×	✓	×
90 to 100 %	×	×	✓	✓

V. Conclusions

This paper analyzed the performance of differential protection functions (87T and 87Q) for converter transformers in the inverter station of HVDC-LCC systems. Internal and external fault scenarios and transformer energization were simulated using an ATP/ATPDraw model of the HVDC Madeira River link, and the response of functions in these scenarios was assessed and reported.

The 87T function performed as expected for energization and external and internal faults on the primary side, effectively protecting the transformers. However, due to undue blocking and restriction by the 2^{nd} harmonic for converter transformers in the same position at the converter of $TFYY_1$ and inadequate fault current sensitivity for converter transformers in the same position at the converter of $TFYD_1$, it exhibited performance failures for single-phase-to-ground and turn-to-ground faults on the DC side. Similarly, the 87Q function was effective in the same scenarios as the 87T and faced the same challenges under faults on the DC side of the $TFYY_1$. Nevertheless, the function showed potential as an alternative for protecting converter transformers similar to $TFYD_1$.

Overall, the differential functions proved reliable for most fault types but revealed the need for enhancements to address unique challenges associated with DC-side faults in converter transformers. Future research should focus on developing improved transformer energization detection methods and designing protection schemes tailored to the specificities of HVDC converter transformers.

References

[1] D. Jovcic and K. Ahmed, *High-voltage Direct-current Transmission: Converters, Systems and DC Grid*, 1st ed. John Wiley & Sons Inc., 2015.
[2] Y. Zhao, “Protection of HVDC Converter Transformers and Role of IEC 61850,” Ph.D. dissertation, University of Manchester, 2018.
[3] P. M. Anderson, C. F. Henville, R. Rifaat, B. Johnson, and S. Meliopoulos, *Power system protection*. John Wiley & Sons, 2022.
[4] X. Lin, J. Lu, Q. Tian, H. Weng, Z. Li, C. Tong, M. Li, J. Sun, and D. Yang, “Abnormal operation behavior analysis and countermeasures on the differential protection of converter transformer,” *International Journal of Electrical Power & Energy Systems*, vol. 64, pp. 516–525, 2014.
[5] T. Zheng, X. Hu, X. Wang, and X. Guo, “Research on the fault-induced inrush current of the converter transformer and its impacts,” in *2018 2nd IEEE Conference on Energy Internet and Energy System Integration (EI2)*. IEEE, 2018, pp. 1–6.
[6] T. Zheng, X. Liu, and X. Guo, “Analysis of fault-induced inrush current of converter transformer in lcc hvdc system considering dc control and protection,” *International Journal of Electrical Power & Energy Systems*, vol. 125, p. 106536, 2021.
[7] T. Zheng, X. Liu, X. Guo, X. Wang, Z. Du, and K. Zhang, “Fault-induced inrush current of inverter-side converter transformer and its impact on differential protection,” 2021.
[8] G. S. Oliveira, C. C. S. Silva, N. S. S. Ribeiro, and K. M. Silva, “HVDC converter transformers protection - part 2: Differential function assessment,” in *2023 Workshop on Communication Networks and Power Systems (WCNPS)*, 2023, pp. 1–7.
[9] J. J. C. Tavares, “Influência de Sistemas HVDC no Desempenho da Proteção de Distância de Linhas de Transmissão CA,” Dissertação de Mestrado em Engenharia Elétrica, University of Brasília, 2020.
[10] G. Sarcinelli, “Model for HVDC training available in ATPDraw/ATP,” 2024, https://www.atpdraw.net/ [Accessed: (2024/11/05)].
[11] Leuven EMTP Center, “ATP-Alternative transient program-rule book,” *Herverlee, Belgium*, 1987.
[12] “EMTP reference models for transmission line relay testing,” *IEEE Power System Relaying Committee*, 2004.
[13] D. G. Hart, D. Novosel, and R. A. Smith, “Modified cosine filters,” *S. Patent*, vol. 6154687, 2000.
[14] *SEL-487E-3,-4 Data Sheet*, Schweitzer Engineering Laboratories, Inc., 2022, available online at https://selinc.com/api/download/99384/.
[15] A. Grid, “Network protection & automation guide,” *Alstom grid*, p. 7, 2011.
[16] IEEE, “Ieee guide for protecting power transformers,” *Proceedings of the IEEE Std C37. 91-2008 (Revision of IEEE Std C37. 91-2000)*, pp. 1–139, 2008.